Invited Paper

III-nitride nanostructures for energy generation

B. N. Pantha, J. Y. Lin, and H. X. Jiang*

Department of Electrical and Computer Engineering, Texas Tech University, Lubbock, Texas 79409, USA

ABSTRACT

Recent developments of III-nitride materials and devices for energy applications such as photovoltaic, thermoelectric, and hydrogen generation are discussed. Although there are only few reports on InGaN based solar cells, some superior properties of this material including radiation tolerance and tunable band gap overlapping with solar spectrum considered it as a suitable candidate for space based and multijuction solar cell. Design and characterization, of InGaN based efficient p-MQW-n solar cells are presented. For the thermopower generation, we discuss the potential of InGaN alloys as thermoelectric material. Good thermoelectric materials possess low thermal conductivity and high Seebeck coefficient with high electrical conductivity. The thermal conductivity about two orders less than that of GaN and thermoelectric figure of merit as good as that of SiGe alloys are measured in $In_{0.36}Ga_{0.64}N$ alloy. Our results indicate that InGaN alloys can be used to convert heat energy directly into electrical energy. Generation of hydrogen by splitting of water using InGaN alloy electrodes and solar energy via photoeletrochemical effect is also discussed

Keywords: solar energy, InGaN, photovoltaic, thermoelectric, water splitting, photolectrochemical effect

1. INTRODUCTION

Present reliance on energy mainly from fossil fuel and its increasing consumption will bring adverse side effects in human health, global warming, and energy crisis in the near future. Finding highly efficient, renewable, and clean source of energy is the single most challenge facing humanity today. At present renewable energy which includes solar, hydroelectric, biomass, geothermal and wind energy supplies only ~7% of total energy demand. III-nitride semiconductors have been successfully used for savings energy through solid state lighting. Additionally, nitride nanostructures hold great promises for energy generation, including applications for thermoelectric, solar cells, and photoelectrochemical cells.

Earth receives tremendous amount of energy from sun. If even a modest fraction of this energy (solar energy) can be converted to electricity, the potential impact on energy efficiency could be enormous, leading to savings in fuel and reductions in carbon dioxide emission. InGaN alloys have been widely exploited as active materials for light-emitting diodes (LEDs) and laser diodes with emission wavelengths covering from near UV to green spectral regions [1-6]. InGaN alloys recently emerge as a new solar cell materials system due to their tunable energy band gaps (varying from 0.7 eV for InN to 3.4 eV for GaN, covering almost the whole solar spectrum) and superior photovoltaic characteristics (direct energy band gap in the entire alloy range and high carrier mobility, drift velocity, radiation resistance, and optical absorption of ~10^5 cm^{-1} near the band edge) [7-11]. InGaN alloys also appear to be an ideal material to split water using sunlight (photoeletrochemical applications) because of their tunable band gap and stability in various electrolytic solutions. Furthermore our recent studies show that thermometric figure of merit of high In content InGaN is reasonably good for thermopower generation.

*hx.jiang@ttu.edu

Quantum Sensing and Nanophotonic Devices VII, edited by Manijeh Razeghi, Rengarajan Sudharsanan, Gail J. Brown, Proc. of SPIE Vol. 7608, 76081I · © 2010 SPIE · CCC code: 0277-786X/10/$18 · doi: 10.1117/12.840726

2. RESULTS

2.1. InGaN/GaN MQW solar cell

Although InGaN based solar cells offer tremendous potential for terrestrial as well as space photovoltaic applications, there are only a few reports on InGaN based solar cells. Furthermore, most reported InGaN solar cells have In contents lower than 15% and band gaps near 3 eV, or larger, and therefore deliver diminishing quantum efficiency at wavelengths longer than 420 nm [7-11]. An earlier theoretical calculation has indicated that the requirements of an active material system to obtain solar cells having solar energy conversion efficiency greater than 50% can be fulfilled by InGaN alloys with In content of about 40%. [12]. Additionally, III-nitride multijunction solar cells with near ideal band gaps for maximum solar energy conversion efficiency must incorporate InGaN layers with higher In contents or lower energy band gaps.

The solar cell layer structure is shown in Fig. 1(a), and the light absorbing region consists of eight periods of $In_xGa_{1-x}N$ (3 nm)/GaN (8 nm) multiple quantum wells (MQWs). The MQWs were grown under the established metal organic chemical vapor deposition (MOCVD) growth conditions of $In_xGa_{1-x}N$ epilayers [13] with targeted x values of 0.3 and 0.4 with the aim of obtaining photovoltaic responses in longer operating wavelengths than previous demonstrations [7-11]. The thickness of p-GaN (n-GaN) epilayer is ~150 nm (~0.5 μm). The device structure was grown on a GaN (3 μm)/sapphire template The PL spectrum for an $In_xGa_{1-x}N$/GaN MQW solar cell structure with the targeted In content of 0.3 is shown in Fig. 1(b) and exhibits an emission line around 472 nm (or ~2.63 eV).

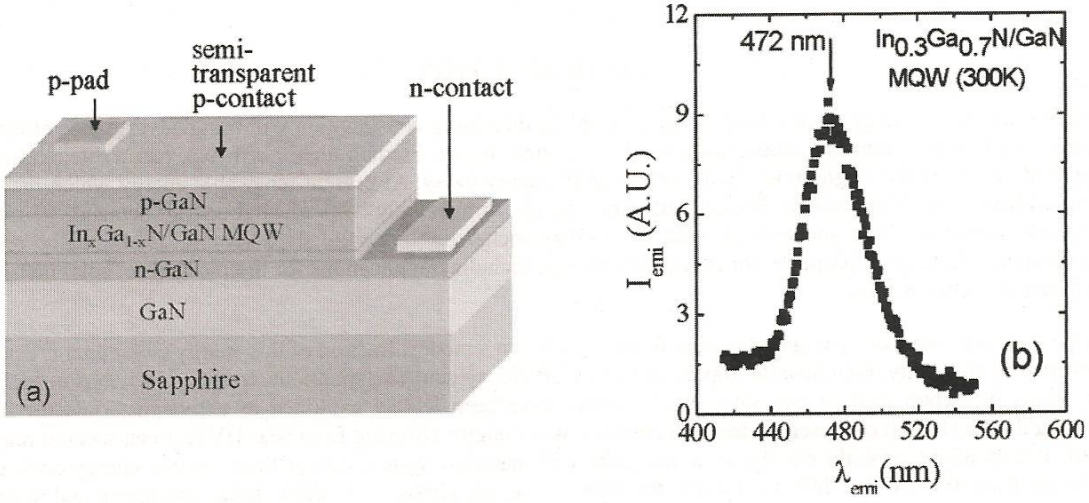

Figure 1. (a) Schematic layer structure of solar cells based on InGaN/GaN MQWs. (b) PL emission spectrum of an $In_xGa_{1-x}N$/GaN MQW (x~0.3) solar cell structure

We adopted the device fabrication steps of commercial III-nitride LEDs by implementing a thin Ni/Au (2/6 nm) semitransparent current spreading layer to minimize the p-contact resistance on the p-GaN window. An optical microscopy image of a fabricated InGaN/GaN MQW solar cell is shown in the inset of Fig. 2(a). For current-density and power-density versus voltage characteristics measurements, the solar cell was illuminated by a white light source (with no optical filter), which has an emission spectrum, as shown in Fig. 2(a). For quantum efficiency versus

excitation wavelength characterization, monochromatic illumination was obtained by using the same white light source in conjunction with a monochromator (with a spectral resolution of about 2.5 nm).

Current versus voltage (*I-V*) characteristics of two fabricated $In_xGa_{1-x}N$/GaN MQW solar cells with targeted In contents (x) of about 0.3 and 0.4 in the well region are shown in Fig. 2(b). The open-circuit voltages (V_{oc}) for devices with x~0.3 and 0.4 are about 2.0 and 1.8 V, respectively. These values are in reasonable agreement with the band gaps of $In_{0.3}Ga_{0.7}N$ and $In_{0.4}Ga_{0.6}N$. However, the performance of the lower energy gap device (with $In_{0.4}Ga_{0.6}N$/GaN MQWs as active region) is poorer than that of the higher energy band gap device (with $In_{0.3}Ga_{0.7}N$/GaN MQWs as active region), despite the fact that $In_{0.4}Ga_{0.6}N$/GaN MQWs are expected to have a much better spectral overlap with the excitation source. This degradation in solar cell performance is a direct consequence of reduced material quality with increasing x, which leads to a higher loss of the photogenerated charge carriers [13]. The photovoltaic characteristics observed here are also consistent with the well established fact that the quantum efficiencies of III-nitride green LEDs are much lower than those of blue LEDs.

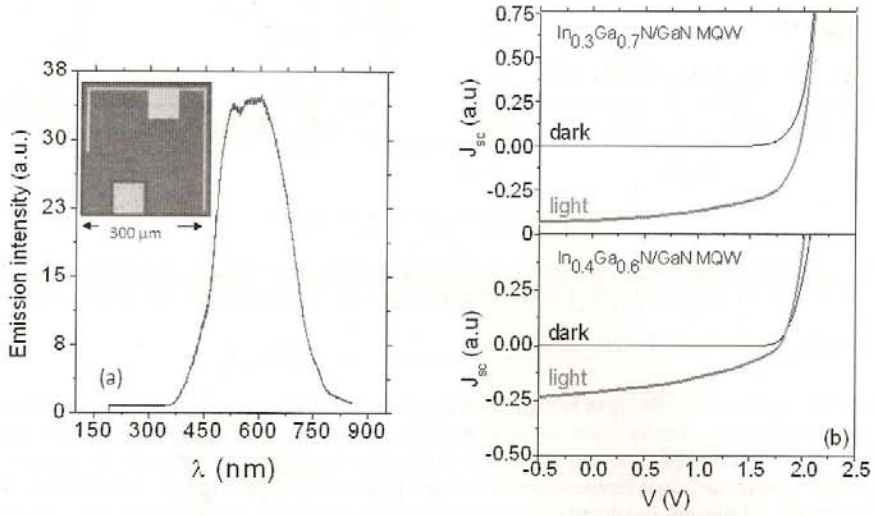

Figure 2. (a) Emission spectrum of the white light source used for current-voltage (*I-V*) characteristics measurements and the inset is an optical microscopy image of a fabricated device. (b) *I-V* characteristics $In_xGa_{1-x}N$/GaN MQW (x~0.3 and 0.4) solar cells

Current-density and power-density versus voltage characteristics for the higher performance device (with $In_{0.3}Ga_{0.7}N$/GaN MQWs as active region) are plotted in Fig. 3(a), from which a fill factor of about 60% is obtained. The quantum efficiency as a function of excitation wavelength for the same device is shown in Fig. 3(b), which demonstrates that the device delivers a quantum efficiency of 40% at 420 nm and 10% at 450 nm. The response in the shorter wavelength region (< 300 nm) is limited by the use of *p*-GaN window [11] and can be improved if a larger band gap material such as *p*-AlGaN or *p*-InAlGaN is incorporated. This is the first demonstration of InGaN based solar cells with good external quantum efficiencies at such long operating wavelengths, which suggest that MQW is a viable approach to design high efficiency solar cells based on InGaN with relatively high In contents for optimal solar energy conversion.

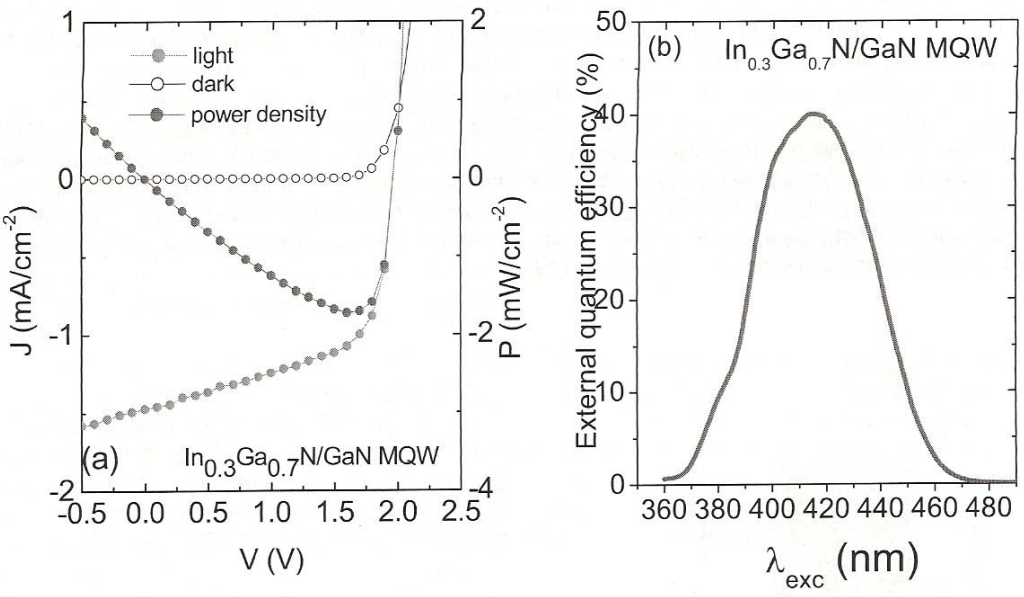

Figure 3. (a) Characteristics of current-density and power-density vs voltage for a solar cell with $In_xGa_{1-x}N$/GaN MQW (x~0.3) as the active region. (b) External quantum efficiency vs excitation wavelength for the same device

2.2. Thermoelectric properties of InGaN alloys

Thermoelectric (TE) devices convert heat energy directly into electrical energy without any moving parts. These devices are environmentally friendly because they produce no ozone-depleting gases and emit no radioactive radiation [14]. Some of the outstanding features of III-nitrides that are highly attractive for TE applications include the ability for high power and high temperature operation, high mechanical strength and stability, and radiation hardness. Additionally, III-nitrides potentially offer tremendous scope for the enhancement of the TE figure of merit (ZT) via alloying, bandgap engineering and nanostructure incorporation with great ease.

The performance of TE materials is characterized by the TE figure of merit (ZT) = S^2T/κ, where S = Seebeck coefficient, σ = electrical conductivity, κ = thermal conductivity, and T = absolute temperature. Since the thermal conductivities of binary III-nitride semiconductors such as InN, GaN, and AlN are so high (> 50 W/m K) that their prospects for TE device applications are limited. However, κ can be significantly reduced in alloys with a very little deterioration of electrical properties making alloy a good candidate as TE materials [15]. Here, we investigate the TE properties of $In_xGa_{1-x}N$ alloys grown by metal organic chemical vapor deposition. We employed 3Ω, temperature gradient, and four probe methods to measure the κ, S, and σ respectively, of InGaN alloys.

Figure 4 shows the variation of κ with x, for $In_xGa_{1-x}N$ alloys measured at 300 K. Results for $Al_xGa_{1-x}N$ (Ref. 16) and $In_xAl_{1-x}N$ (Ref. 17) alloys are also included for comparison. Solid lines are obtained from formula for κ of ternary alloys outlined in reference [15]. A significant reduction in κ of $In_xGa_{1-x}N$ alloys with increasing x is observed, which is mainly attributed to the scattering of phonons due to the alloy disorder [15]. The κ values of $In_xGa_{1-x}N$ alloys are comparable to those of other nitride systems, such as $In_xAl_{1-x}N$ and $Al_xGa_{1-x}N$.

Figure 5(a) shows the measured S and σ of $In_xGa_{1-x}N$ alloys as functions of In content ($0 < x < 0.36$) decreases while σ increases with an increase of x. The reason for this trade-off relationship between S and σ is due the increased electron concentration with an increase of x in $In_xGa_{1-x}N$ alloys. In Fig. 5(b), we plot the power fac ($P = S^2\sigma$) and ZT as functions of In content. Both P and ZT are observed to increase with x. At 300 K, $ZT = 0.08$ obtained in the $In_{0.36}Ga_{0.64}N$ alloy, which is much larger than those in AlInN (Ref. 17) and AlGaN (Ref. 18) alloys which ZT is around (or even smaller than) 0.001 at 300 K. This may be due to the fact that electron mobility InGaN is much higher than that of AlGaN or AlInN

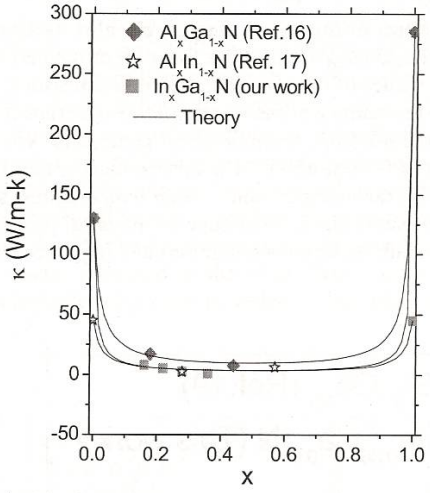

Figure 4. Thermal conductivity (κ) of $In_xGa_{1-x}N$ alloys as a function of In content (x) at 300 K. Data points for AlGa and InAlN (from Refs. 16 and 17) are included for comparison

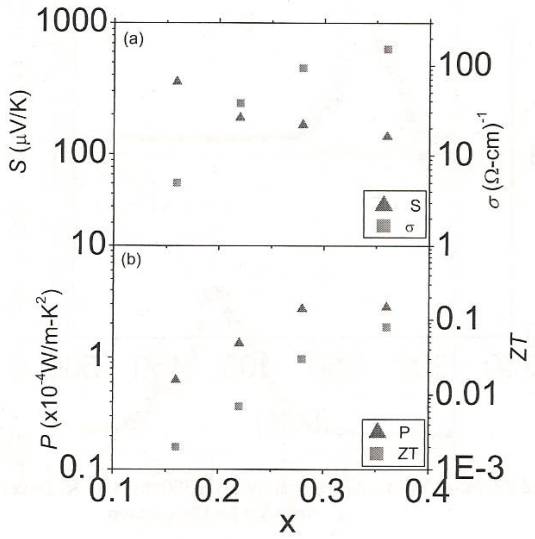

Figure 5. (a) The Seebeck coefficient (S) and electrical conductivity (σ) of $In_xGa_{1-x}N$ alloys as functions of In conten (x). (b) Power factor ($P=S^2\sigma$) and figure of merit (ZT) of $In_xGa_{1-x}N$ alloys as functions of In content (x) measured at 300 K.

The temperature dependent TE properties of $In_xGa_{1-x}N$ alloys were also measured in the temperature range from 300 to 450 K. Figure 6 shows *ZT* of $In_{0.36}Ga_{0.64}N$ alloy as a function of temperature. Data for SiGe alloys [19] are also included for comparison. The *ZT* values of $In_{0.36}Ga_{0.64}N$ alloy in the measured temperature range are comparable to those of the SiGe alloys, which is the current prime choice of TE materials for thermopower generation in high temperature environment such as in radio-isotope thermoelectric generators. We observe that *ZT* increases linearly with temperature and reaches a value of 0.23 at 450 K. The results suggest that $In_xGa_{1-x}N$ alloys may replace SiGe alloys for applications of prolonged TE device operation at high temperatures, such as for recovery of waste heat from automobile, aircrafts, and power plants due to their superior physical properties over those of SiGe, including the ability of operating at high temperature/high power conditions and high mechanical strength and stability.

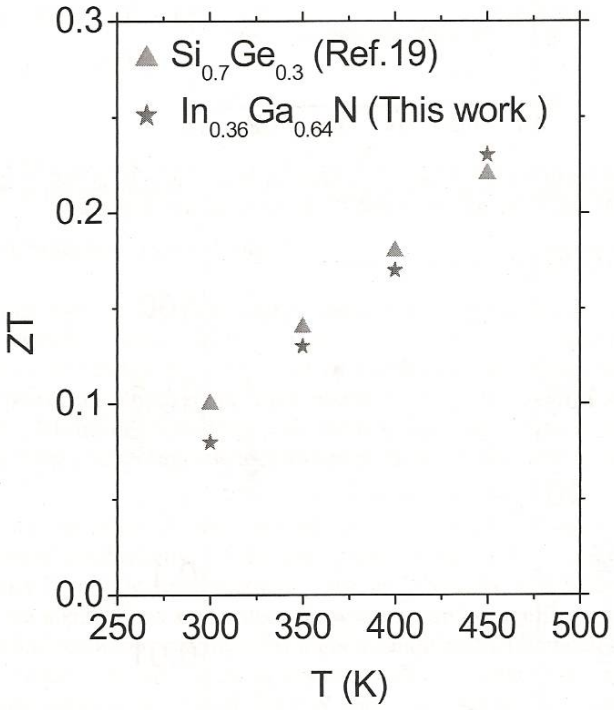

Figure 6. Measured *ZT* values of $In_{0.36}Ga_{0.64}N$ alloy from 300 to 450 K. Data for SiGe alloys from Ref. 19 are included for comparison.

2.3. Photoelectrochemical effect of InGaN alloys and hydrogen generation

Currently, the most favored material for the photoanode in PEC is TiO_2 due to its high corrosion resistance [20]. However, TiO_2 has an energy bandgap of about 3.2 eV and can only be activated by light energy equal to or greater than 3.2 eV. Such energy range is unfortunately present in less than 3% of the solar spectrum. This results in

very low solar absorptivity in TiO_2. Henceforth, they are intrinsically insufficient (<2%) in systems for solar energy conversion such as in PEC [20]. Considering the general science and engineering requirements, InGaN appears to be an ideal material for the development of next generation PEC because of their ability of absorbing entire solar spectrum via bandgap engineering such as alloying and nanostructure formation [8]. Additionally, the smaller lattice constants or stronger bonding of In–N and Ga–N of III nitrides compared with other semiconductors (GaP, for example) also implies higher corrosion resistance, however, very little work has been done with respect to their potential for electrolyzing water [21-24].

The $In_xGa_{1-x}N$ electrodes used in water splitting experiment were grown on 1.5 μm thick GaN/sapphire templates by MOCVD. The thickness of InGaN layer was 0.2 μm. The typical room temperature electron concentration and mobility of InGaN alloys were 2×10^{17} cm^{-3} and 160 cm^2/Vs, respectively, as determined by Hall effect measurements. Figure 7 shows the room temperature PL spectra of two $In_xGa_{1-x}N$ epilayers used for water splitting experiments, where samples 1 and 2 have In contents of about 0.2 and 0.4, respectively, which were determined by x-ray diffraction. Although the overall PL emission intensity of sample 2 is lower than that of sample 1 due to its reduced crystalline quality with increasing In content, the bandgap of sample 2 with an emission peak around 2.1 eV matches better with the solar spectrum. The water splitting efficiencies of photocatalytic electrodes based upon InGaN materials were measured using a standard photoelectrochemical cell. The cell consists of a working electrode (InGaN), a cathode (Pt counter electrode), and a sodium-chloride-saturated calomel silver-chloride electrode. The electrodes were immersed in the electrolyte solution. The potential difference (voltage) between the working and counter electrodes (V_{CE}) was recorded to determine the applied bias and the photocurrent (I_p) was measured as a function of V_{CE}.

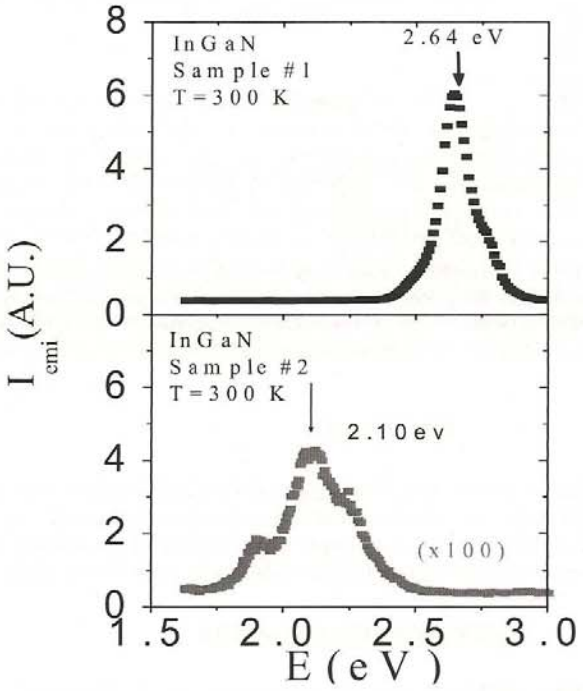

Figure 7. Room temperature photoluminescence spectra of two *n*-$In_xGa_{1-x}N$ epilayers (with x~0.2 and 0.4) used in water splitting experiments.

We have obtained preliminary results by employing InGaN epilayers as working electrodes. We have measured the photocurrent density as a function of V_{CE} by using samples 1 and 2 as working electrodes and plotted in Fig. 8. The experimental set up is shown in Fig. 9. Under white light illumination, a drastic dependence of the photocurrent density on the In content was observed. Sample 2 with lower PL emission energy (or higher In content) provides much higher photocurrent density. Since the overall material quality of sample 2 (x~0.4) is lower than that of sample 1 (x~0.2), the higher performance (higher photocurrent density) of sample 2 is solely due to the greater overlap of its energy bandgap with the solar spectrum. Furthermore, as shown in Fig. 9, when sample 2 was immersed in 1 M HCl, H_2 evolved vigorously from the Pt counter electrode.

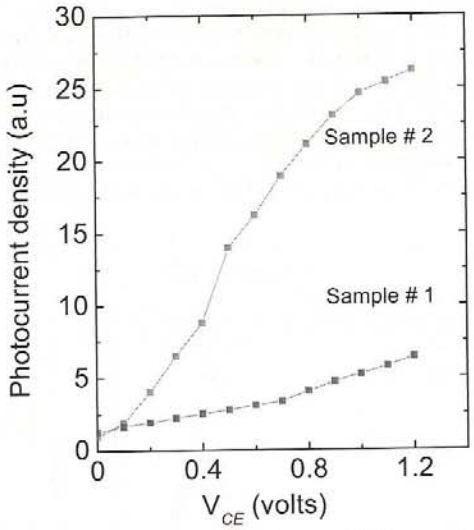

Figure 8. Photocurrent density vs V_{CE} (the bias voltage applied between the working and counter electrodes) of InGaN based PEC. The results were obtained in aqueous 1 mol HCl under static condition and white light illumination by using 2 different n-$In_xGa_{1-x}N$ epilayers (with x=0.2 and 0.4) as working electrodes (1×1 cm^2). H_2 generation is only visible when using sample 2.

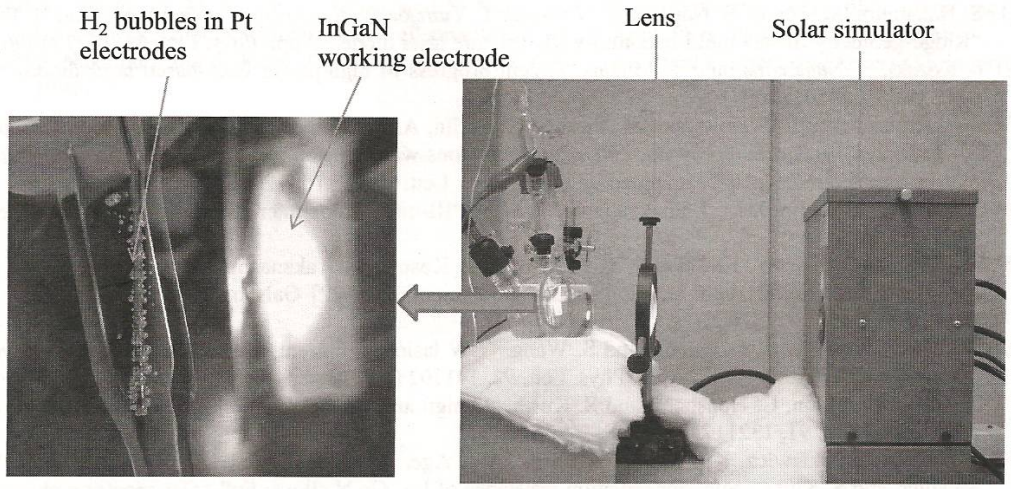

Figure 10. A photograph of experimental set-up for PEC experiments. Hydrogen gas (H_2 gas bubbles) generation on the Pt counter electrode side through water splitting accomplished using an *n*-type $In_{0.4}Ga_{0.6}N$ epilayer as a working electrode under white light illumination is clearly shown in the left picture.

Our results suggest that the estimated In composition in InGaN as a photocatalytic electrode for optimal photoelectrolysis of water should be above 0.4. However, as we tune into the miscibility gap region in InGaN alloys with InN fraction between 45%–60%, [25] optimal effective composition will need to be determined by several complementary techniques due to the well known formation of In-rich nanoclusters (or quantum dots) [26,27] in the middle composition range. On the other hand, this spontaneous formation of nanoclusters in InGaN may be highly effective in increasing the water splitting efficiency. Furthermore, there is no visible physical degradation of the InGaN epilayers after several hours of measurements. InGaN based PEC cells are expected to provide superior corrosion resistance due to the small lattice constants and strong bonding between In/Ga and N. However, prolonged measurements are needed to further study the corrosion effect and to verify this potential. Nevertheless, we believe that this demonstration of hydrogen generation by water splitting accomplished using sunlight using InGaN based PEC is highly promising.

SUMMARY

In summary we have demonstrated that InGaN alloys hold promises as potential candidates for future energy generation using photovoltaic, thermoelectric, and photo-electrolysis technologies. Additionally, these results indicate that efficient devices can be realized with improved quality of high In content InGaN alloys. Therefore, much attention has to given to find ways of synthesizing high quality high In content InGaN alloys.

ACKNOWLEDGEMENTS

H. X. Jiang and J. Y. Lin would like to acknowledge the support of NSF (DMR-0906879, ECCS-0854619), and ARO. They also gratefully acknowledge the support of the Edward Whitacre and Linda Whitacre endowment chair positions through the AT & T Foundation. Contributions from their group members are also acknowledged

REFERENCES

[1] S. Nakamura, M. Senoh, S. Nagahama, N. Iwasa, T. Yamada, T. Matsushita, Y. Sugimoto, and H. Kiyoku, "Ridge-geometry InGaN multi-quantum-well-structure laser diode," Appl. Phys. Lett. **69**, 1477 (1996).
[2] T. Kozaki, S. Nagahama, and T. Mukai, "Recent progress of high-power GaN-based laser diodes," Proc. SPIE **6485**, 648503 (2007).
[3] C. Skierbiszewski, P. Wiśniewski, M. Siekacz, P. Perlin, A. Feduniewicz-Zmuda, G. Nowak, I. Grzegory, M. Leszczyński, and S. Porowski, "60 mW continuous-wave operation of InGaN laser diodes made by plasma-assisted molecular-beam epitaxy," Appl. Phys. Lett. **88**, 221108 (2006).
[4] H. X. Jiang, S. X. Jin, J. Li, J. Shakya, and J. Y. Lin, "III-nitride blue microdisplays," Appl. Phys. Lett. **78**, 1303 (2001).
[5] M. Funato, M. Unde, Y. Kawakami, Y. Narukawa, T. Kosugi, M. Takanashi, and T. Mukai, "Blue, green, and amber InGaN/GaN light-emitting diodes on semipolar [11-22] GaN bulk substrates," Jpn. J. Appl. Phys., Part 2 **45**, L659 (2006).
[6] T. Lu, C. Kao, H. Kuo, G. Huang, and S. Wang, "CW lasing of current injection blue GaN-based vertical cavity surface emitting laser," Appl. Phys. Lett. **92**, 141102 (2008).
[7] O. Jani, I. Ferguson, C. Honsberg, and S. Kurtz, "Design and characterization of GaN/InGaN solar cells," Appl. Phys. Lett. **91**, 132117 (2007).
[8] J. Wu, W. Walukiewicz, K. M. Yu, W. Shan, J. W. Ager III, E. E. Haller, H. Lu, W. J. Schaff, W. K. Metzger, and S. Kurtz, "Superior radiation resistance of $In_{1-x}Ga_xN$ alloys: Full-solar-spectrum photovoltaic material system," J. Appl. Phys. **94**, 6477 (2003).
[9] Y. Nanishi, Y. Satio, and T. Yamaguchi, "RF-molecular beam epitaxy growth and properties of InN and related alloys," Jpn. J. Appl. Phys. Part 1 **42**, 2549 (2003).
[10] M. Vazquez, C. Algora, I. Rey-Stolle, and J. R. Gonzalez, "III-V concentrator solar cell reliability prediction based on quantitative LED reliability data," Progr. Photovoltaics **15**, 477 (2007).
[11] C. J. Neufeld, N. G. Toledo, S. C. Cruz, M. Iza, S. P. DenBaars, and U. K. Mishra, "High quantum efficiency InGaN/GaN solar cells with 2.95 eV band gap," Appl. Phys. Lett. **93**, 143502 (2008).
[12] A. De Vos, *Endoreversible thermodynamics of solar energy conversion* (Oxford University Press, Oxford, 1992), p. 90.
[13] B. N. Pantha, J. Li, J. Y. Lin, and H. X. Jiang, "Single phase $In_xGa_{1-x}N$ ($0.25 \leq x \leq 0.63$) alloys synthesized by metal organic chemical vapor deposition", Appl. Phys. Lett. **93**, 182107 (2008).
[14] G. Mahan, B. Sales, and J. Sharp, "Thermoelectric materials: new approaches to an old problem", Phys. Today **50**, 42 (1997).
[15] G. S. Nolas, J. Sharp, and H. J. Goldsmid, *Thermoelectrics Basic Principles and New Materials Development*, Springer Series in Material Science Vol. 45 (Springer, New York, 2001)
[16] B. C. Daly, H. J. Maris, A. V. Nurmikko, M. Kuball, and J. Han, "Optical pump-and-probe measurement of the thermal conductivity of nitride thin films," J. Appl. Phys. **92**, 3820 (2002).
[17] S. Yamaguchi, R. Izaki, K. Yamagiwa, K. Taki, Y. Iwamura, and A. Yamamoto, "Thermal diffusivity and thermoelectric figure of merit of $Al_{1-x}In_xN$ prepared by reactive radio-frequency sputtering," Appl. Phys. Lett. **83**, 5398 (2003).
[18] W. Liu and A. A. Balandin, "Thermoelectric effects in wurtzite GaN and $Al_xGa_{1-x}N$ alloys," J. Appl. Phys. **97**, 123705 (2005).
[19] J. P. Dismukes, L. Ekstrom, E. F. Steigmeier, I. Kudman, and D. S. Beers, "Thermal and Electrical Properties of Heavily Doped Ge-Si Alloys up to 1300°K," J. Appl. Phys. **35**, 2899 (1964).
[20] A. J. Nozik and R. Memming, "Physical Chemistry of Semiconductor−Liquid Interfaces," J. Phys. Chem. **100**, 13061 (1996).
[21] S. S. Kocha, M. W. Peterson, D. J. Arent, J. M. Redwing, M. A. Tischler, and J. Turner, "Electrochemical Investigation of the Gallium Nitride-Aqueous Electrolyte Interface," J. Electrochem. Soc. **142**, L238 (1995).
[22] K. Fujii, T. Karasawa, and K. Ohkawa, "Hydrogen Gas Generation by Splitting Aqueous Water Using n-Type GaN Photoelectrode with Anodic Oxidation," Jpn. J. Appl. Phys. Part 2 **44**, L543 (2005).
[23] K. Fujii and K. Ohkawa," Photoelectrochemical properties of p-type GaN in comparison with n-type GaN," Jpn. J. Appl. Phys., Part 2 **44**, L909 (2005).
[24] I. Waki, D. Cohen, R. Lal, U. Mishra, S. P. DenBaars, and S. Nakamura, " Direct water photoelectrolysis with patterned *n*-GaN," Appl. Phys. Lett. **91**, 093519 (2007).
[25] I. H. Ho and G. B. Stringfellow, "Solid phase immiscibility in GaInN," Appl. Phys. Lett. **69**, 2701 (1996).

[26] S. Nakamura, M. Senoh, N. Iwasa, and S. Nagahama, "High-brightness InGaN blue, green and yellow light-emitting diodes with quantum well structures," Jpn. J. Appl. Phys. Part 2 **34**, L797 (1995).
[27] S. Nakamura and G. Fasol, *The Blue Laser Diode: GaN Based Light Emitters and Lasers* (Springer, Berlin, 1997).

PROCEEDINGS OF SPIE

Quantum Sensing and Nanophotonic Devices VII

Manijeh Razeghi
Rengarajan Sudharsanan
Gail J. Brown
Editors

24–28 January 2010
San Francisco, California, United States

Sponsored and Published by
SPIE

Volume 7608

Proceedings of SPIE, 0277-786X, v. 7608